ANTIOXIDANTS & REDOX SIGNALING
Volume 13, Number 2, 2010

DOI: 10.1089/ars.2009.2832

ORIGINAL RESEARCH COMMUNICATION

DJ-1 Loss by Glutaredoxin but Not Glutathione Depletion Triggers Daxx Translocation and Cell Death

Uzma Saeed,* Ajit Ray,* Rupanagudi Khader Valli,
A. Madan Ram Kumar, and Vijayalakshmi Ravindranath†

Abstract

Environmental and genetic causes are implicated in the etiopathogenesis of Parkinson's disease (PD), a neurodegenerative movement disorder. DJ-1, a putative gene recessively linked to early onset PD, functions as an antioxidant, transcriptional co-activator, and molecular chaperone. We examined DJ-1 status following global perturbation of protein thiol homeostasis by depleting cellular antioxidant glutathione or downregulating glutaredoxin 1, a thiol disulfide oxidoreductase, wherein both paradigms generate oxidative stress. While these perturbations did not affect expression of DJ-1 mRNA, downregulation of glutaredoxin 1 but not glutathione depletion caused loss of DJ-1 protein, translocation of Daxx (a death-associated protein) from nucleus, and cell death. Overexpression of wild-type DJ-1, but not the cysteine mutants, prevented Daxx translocation and cytotoxicity. Protease inhibitors prevented constitutive DJ-1 loss. Residual DJ-1 was present in reduced state, indicating that DJ-1 when oxidized was degraded through proteolysis. Thus, loss of DJ-1 occurring through its oxidative modification and subsequent proteolysis mediated through dysregulation of thiol disulfide oxidoreductase may contribute to pathogenesis of sporadic PD, thus providing a link between environmental challenges and constitutive levels of this vital protein. *Antioxid. Redox Signal.* 13, 127–144.

Introduction

OXIDATIVE STRESS MAY BE DEFINED as a state wherein there is an imbalance in generation of oxidizing entities and their neutralization by antioxidant defense systems in the cell. One of the consequences of oxidative stress is perturbation of thiol homeostasis, which leads to modification of critical thiol groups of proteins. Oxidative modifications of protein thiol groups can regulate function in reversible or irreversible ways and are now recognized as an important signaling mechanism. Disruption of this balance is implicated in the pathogenesis of neurodegenerative diseases, such as stroke, Alzheimer's disease, and Parkinson's disease (PD) (3, 9, 30).

PD is a progressive degenerative movement disorder resulting from the selective degeneration of dopaminergic neurons in the substantia nigra pars compacta (SNpc) in the ventral midbrain. PD is primarily sporadic in incidence, and oxidative stress, mitochondrial dysfunction, and dysregulation of protein turnover machinery have been suggested as possible mechanisms underlying the selective degeneration. A small percentage of cases are familial and genes putatively linked to this class of PD include DJ-1, α-synuclein, PINK1, Parkin, Lrrk2, HtrA2/Omi, and ATP13A2 (5). Understanding the function of these genes in normal and diseased states has provided insights into the pathogenesis of PD. Dysregulation of these genes and their protein products could also occur by mechanisms distinct from genetic mutations seen in familial PD. Understanding such mechanisms would help us to describe the pathogenic mechanisms underlying sporadic PD.

DJ-1 is one of the putative genes linked to recessive familial form of PD. Loss of function mutations, such as deletion, truncation, and point mutations L166P, M26I, E64D (18) in the DJ-1 locus account for 1%–2% of early onset PD. Studies using loss of function mutations have suggested various functions for DJ-1, such as an antioxidant, a transcriptional co-activator, and/or a molecular chaperone. We examined the status of the DJ-1 protein under different oxidant stressors with a rationale to understand the critical role of DJ-1 in protection against oxidative stress and the potential consequence thereof with respect to the pathogenesis of sporadic PD.

DJ-1 helps in scavenging reactive oxygen species (ROS) and thereby maintains the redox status of proteins (28, 31, 37). DJ-1 has multiple cysteine residues, the oxidation of which enables it to act as a redox sensor during oxidative stimuli, such as exposure to hydrogen peroxide or paraquat (31, 47). Synthetic

Division of Cellular and Molecular Neurosciences, National Brain Research Centre, Nainwal Mode, Manesar, India.
*These authors contributed equally to the work.
†*Current affiliation:* Centre for Neuroscience, Indian Institute of Science, Bangalore, India.

mutations of the cysteines at positions 46, 53, and 106 have provided an understanding of the mechanism underlying the cytoprotection offered by DJ-1 in response to oxidative stress. It adds increasing numbers of oxygen atoms to its cysteine sulfhydryl groups, leading to alteration in its localization and function.

Studies with synthetic mutations of DJ-1 suggest C106 to be the most vulnerable site for oxidation when compared to C46 and C53. C106 is reversibly modified to sulfenic acid (R-S-OH) when exposed to oxidative stimuli, such as hydrogen peroxide, rotenone, or MPP^+(8, 26). The C106A mutation also restricts its translocation to mitochondria and subsequent protection against oxidative stress (8).

Protein thiol homeostasis is critical for the normal functioning of the proteins and may be perturbed in presence of oxidative insult. Cells harbor different antioxidant systems to regulate redox environment. The most abundant cellular thiol antioxidant, glutathione (GSH), can scavenge oxidative species directly. An essential mode of regulation of proteins is glutathionylation, wherein glutathione reversibly associates with thiol groups of proteins to form mixed protein–glutathione disulfides 'Pr-SSG' (30). Thiol disulfide oxidoreductases (TDORs) are responsible for protecting and/or modulating protein function primarily by reducing thiol disulfides.

TDORs include glutaredoxins and thioredoxins—both cytosolic and mitochondrial. Cytosolic glutaredoxin (Grx1) exhibits both glutathionylation and deglutathionylation activities, the latter being explored and reported more. However, Grx1 accelerates the uncatalyzed glutathionylation reaction, thus providing an evidence for glutatathionylating properties (17). Glutaredoxins act via two redox active cysteines (CXXC motif; CPYC in case of Grx1; thiolate at physiological pH) by attacking the glutathionyl sulfur of Pr-SSG or the disulfide bond of oxidized substrate (Pr-SS-Pr). This results in formation of glutathionyl enzyme mixed disulfide (Grx-SSG) and release of reduced protein thiol (Pr-SH). Grx-SSG can either form reduced Grx in the presence of GSH or an intramolecular disulfide form of the enzyme, which is further reduced by GSH and recruited back into the catalytic cycle (17). Grx1 activity is maintained by glutathione reductase utilizing reducing equivalents from NADPH and GSH (19). Grx1 can either transiently act as a glutathionylating enzyme in presence of an oxidative stimulus (13) or as a deglutathionylase when oxidative stress subsides, thereby stabilizing proteins during oxidative stress and preventing their irreversible modification (11).

In this study, we examined the effect of perturbation of the thiol homeostasis either by Grx1 downregulation or cellular GSH depletion on DJ-1. We found differential effects on DJ-1 upon global redox modulation through GSH loss and a more specific perturbation of TDORs in the form of Grx1 knockdown.

Materials and Methods

Materials

2′,7′-Dichlorodihydrofluorescein diacetate (H_2DCFDA) and MitoTracker were purchased from Molecular Probes (Eugene, OR); L-buthionine-S-R-sulfoximine (BSO) from Chemical Dynamics Corporation (South Plainfield, NJ). Dithiobisnitrobenzoic acid (DTNB), 5-sulfosalicylic acid, N-acetyl cysteine (NAC), and nicotinamide adenine dinucleotide phosphate (reduced; NADPH) were obtained from Sigma (St. Louis, MO). α-Lipoic acid was procured from Fluka Chemicals (Buchs, Switzerland). Antibodies to Grx1 and Trx1 were obtained from Lab Frontiers Life Science Institute (Seoul, Korea). Trx1 antibody cross-reacts with both Trx1 and Trx2 and we thus report only Trx expression. Antibodies to DJ-1, Daxx, and SOD-1 were obtained from Santa Cruz Biotechnology Inc. (Santa Cruz, CA). Antibodies to β-tubulin and FLAG were obtained from Sigma (Milwaukee, WI). *In situ* Cell Death Detection Kit, TMR red, was obtained from Roche Diagnostics GmbH (Indianapolis, IN). Cell culture products and Lipofectamine™ were obtained from Invitrogen (Carlsbad, CA). All other chemicals and reagents were of analytical grade and were obtained from Sigma Chemical Company (St. Louis, MO) or Merck (India).

Cell culture and treatment

Neuro-2a, SH-SY5Y, and COS-7 cells (all from American Type Culture Collection, Manassas, VA) were cultured in DMEM, supplemented with 10% (v/v) fetal bovine serum, 100 units/ml penicillin G, and 100 mg/ml streptomycin. Cells were treated with either buthionine sulfoximine (BSO; 100 μM) or vehicle (0.9% saline) 24 h following seeding. Medium containing BSO was replaced every 24 h and the treatment culminated at 48 h, after which cells were collected and processed for either estimation of total glutathione or RNA and protein extraction.

Downregulation of Grx1

Oligonucleotides coding for shRNA (Grx1) were annealed and cloned into mU6pro vector kindly provided by Prof. D. Turner (Univ. of Michigan, Ann Arbor) prior to transfection. Nontargeting scrambled sequence for shRNA to Grx1 was also cloned similarly into mU6pro vector and used as a control. Empty vector (mU6pro) was also used as control. Oligonucleotide sequences for shRNA to Grx1 were 5′-TTT GCG GAT GCA GTG ATC TAA TAA GTT CTC TAT TAG ATC ACT GCA TCC GCT TTT T–3′ and 5′-CTA GAA AAA GCG GAT GCA CTG ATC TAA TAG AGA ACT TAT TAG ATC ACT GCA TCC G-3′, and for the scrambled were 5′-TTT GTT GGT TAC GGG GTA TCG ATT CAA GAG ATC GAT ACC CCG TAA CCA ACT TTT T-3′ and 5′-CTA GAA AAA GTT GGT TAC GGG GTA TCG ATC TCT TGA ATC GAT ACC CCG TAA CCA A-3′. Transfections were carried out using Lipofectamine according to manufacturer's protocol. In some experiments (Figs. 1A and 2A) the silencing cassette from mU6pro vector was subcloned into pAAV-GFP (Stratagene), generating pAAV-GFP-shRNA and used for transfections. Cells were harvested 72 h after transfection and expression of the target gene (Grx1) was analyzed at the protein level by immunoblotting and immunostaining and at the mRNA level by qRT-PCR to confirm knockdown of Grx1. In order to observe the effect of time-dependent loss of Grx1 on DJ-1 status, Neuro-2a cells were transfected with either scrambled or shRNA to Grx1 and harvested 24, 48, or 72 h later. In order to examine the gene dose-dependent loss of DJ-1, Neuro-2a cells were transfected with either scrambled (1.0 units) or shRNA to Grx1 (0.5, 1.0, and 1.5 units) for 48 h to reduce effects of cytotoxicity of higher dose. Plasmid dose of '1.0 unit' corresponds to the amount of plasmid used in all other single transfection experiments.

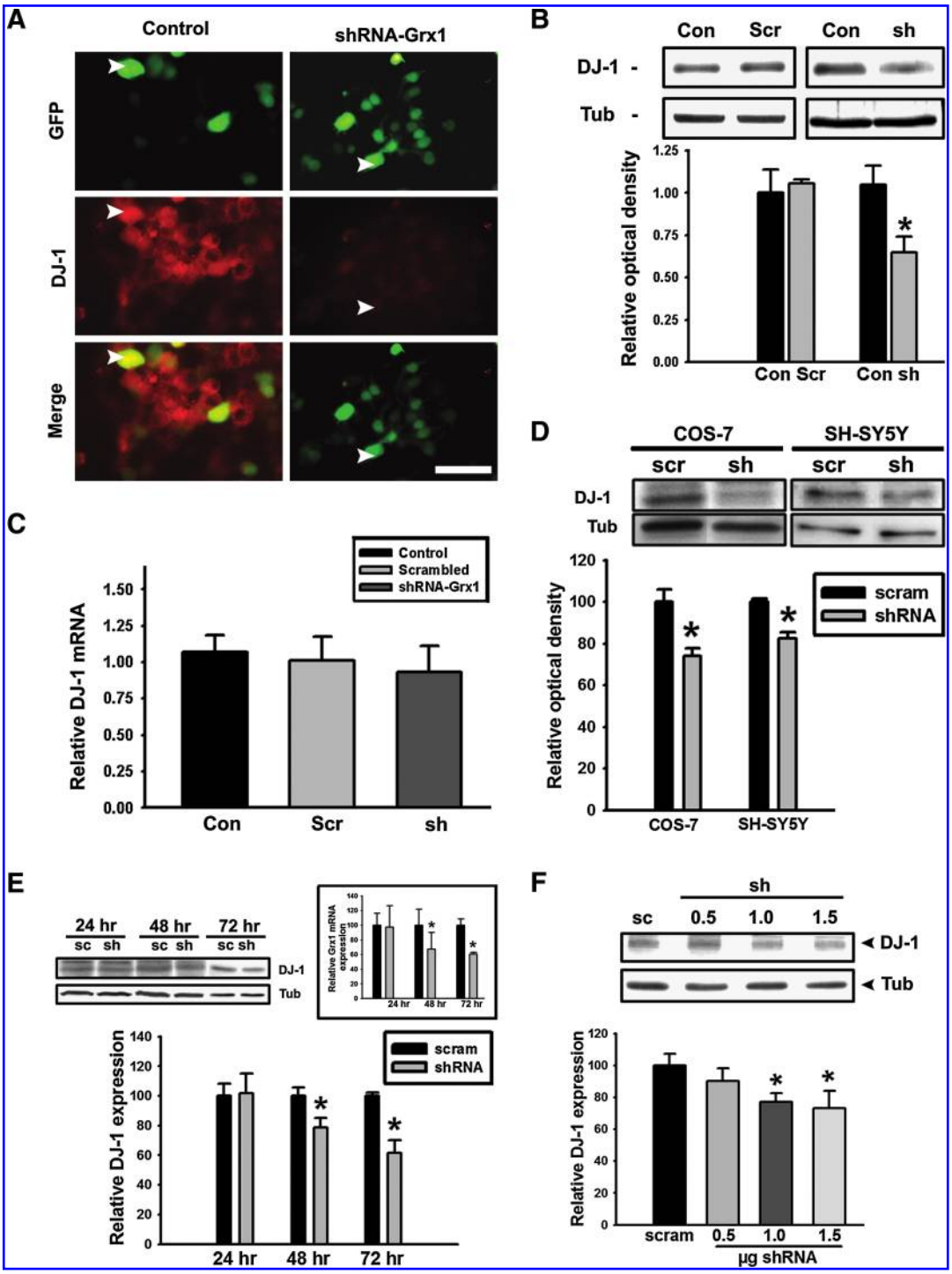

FIG. 1. Grx1 knockdown alters DJ-1 protein levels but not mRNA. Neuro-2a cells transfected with pAAV-GFP (control) or pAAV-GFP-shRNA (shRNA-Grx1) were immunostained for DJ-1. (**A**) GFP expression represents transfected cells; shRNA-Grx1 (*lower panel*) causes decreased expression of DJ-1 compared to GFP expressing control (*upper panel*). *Bar* represents 100 μm. (**B, C**) Neuro-2a cells transfected with either mU6-shRNA or scrambled to Grx1 or empty vector were collected and processed for immunoblotting and qRT-PCR. (**B**) Representative immunoblot showing decrease in protein levels of DJ-1 caused by shRNA to Grx1. ($n = 5$; $p < 0.001$). (**C**) Unaltered mRNA levels of DJ-1 as depicted by qRT-PCR of cells transfected with Grx1 shRNA or scrambled or empty vector ($n = 4$). (**D**) SH-SY5Y and COS-7 cells transfected with either mU6-shRNA to Grx1 also show decrease in DJ-1 protein levels caused by shRNA to Grx1 compared to scrambled transfected control ($n = 3$; $p < 0.01$). (**E**) Progressive loss of DJ-1 protein and Grx1 mRNA knockdown (*inset*) at 24, 48, and 72 h of transfection ($n \geq 4$; $p < 0.05$ for 48 and 72 h). (**F**) Progressive loss of DJ-1 protein in a gene dose-dependent manner following transfection for 48 h with 0.5, 1.0, and 1.5 units of mU6-shRNA plasmid or 1.0 unit of scrambled control ($n = 3$; $p < 0.05$ for 1.0 and 1.5). (For interpretation of the references to color in this figure legend, the reader is referred to the web version of this article at www.liebertonline.com/ars).

Overexpression of DJ-1 in Neuro-2a cells

Constructs overexpressing N-terminal FLAG-tagged wild-type (WT) human DJ-1, and mutants (C106A, C53A, L166P) in pcDNA 3.1 were provided as a kind gift from Prof. Tak W. Mak (The Campbell Family Institute for Breast Cancer Research, ON, Canada) and Prof. David S. Park (Univ. of Ottawa, ON, Canada). Neuro-2a cells were transiently co-transfected with DJ-1 overexpressing constructs (wild type or mutants), along with either shRNA or scrambled to Grx1, as per the requirement of the experiment using Lipofectamine. Cells in control group were cotransfected with scrambled construct and respective backbone vector, ensuring that each group was cotransfected with two plasmids in equal amounts. Cells were collected 72 h post transfection for qRT-PCR and immunoblotting or fixed on chamberslides for immunostaining or cell death assay (TUNEL).

Treatment of cells with α-lipoic acid or N-acetyl cysteine

In some experiments Neuro-2a cells were treated with α-lipoic acid (ALA; 100 μM dissolved in DMSO) 6 h following transfection with either scrambled or shRNA to Grx1 and the cells were harvested 72 h later, with replacement of ALA in fresh medium every 24 h. Alternatively, N-acetyl cysteine (NAC; 0.5 m*M* and 1 m*M* dissolved in 0.9% saline) was added for the last 24 h of the experiment while the cells were harvested at 72 h following transfection and analyzed for DJ-1 by immunoblotting. DMSO and saline were used as vehicles for ALA and NAC respectively.

Treatment of cells with protease or proteasome inhibitors

Following transfection with scrambled or shRNA to Grx1 constructs, proteasome inhibitor MG132 (10 μM) was added to cells 0 or 7 h prior to harvesting at the end of 48 h. Cells were also co-transfected with FLAG-tagged WT human DJ-1 along with shRNA or scrambled construct and then treated with MG132 (10 μM) or dimethyl sulfoxide (DMSO) for 7 h, 41 h post transfection. Nontreated (NT) cells were harvested at 41 h. For protease inhibition experiments, similar transfections were carried out and the cells were treated with 0.05% DMSO or protease inhibitor cocktail giving a final concentration of 52 μM 4-(2-aminoethyl) benzenesulfonyl fluoride, 40 n*M* aprotinin, 2 μM bestatin, 700 n*M* E-64, 1 μM leupeptin, and 750 n*M* pepstatin A for 48 h, with replacement of inhibitors in fresh medium every 12 h.

Intracellular ROS measurement

The oxidant-sensitive dye 2′,7′-dichlorodihydrofluorescein diacetate (H_2DCFDA) was used to measure intracellular ROS. For qualitative determination of ROS levels, cells were seeded at 60% confluency 24 h prior to transfection with shRNA to Grx1 or empty vector. Cells were loaded with 10 μM H_2DCFDA (in DMSO) 72 h following transfection and kept for 15 min at 37°C. They were then rinsed in PBS and viewed under an inverted fluorescence microscope. For quantitative measurement of intracellular ROS cells were incubated with H_2DCFDA for 45 min, washed with PBS, and lysed in ice-cold lysis buffer (potassium phosphate buffer containing 4 *M* NaCl, 0.5 *M* EDTA, 0.5 *M* EGTA, 1% Igepal, protease inhibitors) and centrifuged at 10,000 rpm for 15 min at 4°C. The supernatant was diluted with PBS and the fluorescence measurements were made at 490 nm (excitation) and 530 nm (emission).

Assay of total glutathione

Cells were lysed in 100 m*M* potassium phosphate buffer containing 1 m*M* EDTA (pH 7.4). Cellular debris was removed by centrifuging at 1000 *g* for 10 min at 4°C. An aliquot of lysate was added to an equal volume of 5-sulfosalicylic acid solution (10% w/v; Sigma), mixed and centrifuged at 10,000 *g* for 10 min at 4°C and the acid-soluble supernatant was used for estimation. Protein concentration of the lysate was estimated by a dye-binding method (6). Total cellular glutathione (GSH + GSSG) in the cell lysate was estimated by an enzymatic recycling method (46) and expressed as nmol glutathione/mg protein.

Preparation of mitochondrial fraction for DJ-1 analysis by immunoblotting

Neuro-2a cells were harvested 72 h post transfection with either scrambled or shRNA to Grx1 and homogenized in 0.1 *M* potassium phosphate buffer (pH 7.4, containing 0.25 *M* sucrose, 1 m*M* EDTA, and protease cocktail inhibitors) using 30 strokes in a Potter–Elvehjem homogenizer. The homogenate was centrifuged at 1000 *g* at 4°C for 10 min. The supernatant was further centrifuged at 13000 *g* at 4°C for 20 min and the pellet was washed with fresh homogenization buffer twice, repeating the centrifugation steps. Finally, the mitochondrial pellet was resuspended in the homogenization buffer and used for immunoblotting.

Immunostaining and colocalization studies

Cells, grown in chamber slides were fixed 72 h after transfection and immunostaining was carried out for Daxx and DJ-1. In experiments performed to assess the mitochondrial localization of DJ-1, the cells were loaded with MitoTracker 3 h prior to fixation and then immunostained for DJ-1. Cells immunostained for Daxx were stained with propidium iodide to label the nucleus. Quantitation for subcellular localization of Daxx and DJ-1 were done by scoring an average of 400 cells each from at least four independent experiments.

Quantitative real-time PCR for assessing expression of Grx1 and DJ-1

Total RNA was isolated from Neuro-2a cells transfected with scrambled or shRNA to Grx1 using RNeasy Mini kit (Qiagen, Germany) and cDNA synthesized using random hexamers. Quantitative real-time PCR (qRT-PCR) was performed using Power SYBR Green PCR Master Mix from Applied Biosystems (Foster City, CA), according to manufacturer's instructions. The sequences of primers used for quantitating levels of Grx1 of mouse origin were 5′-TCC TCA GTC AAC TGC CTT TCA-3′ (Grx1-forward), 5′-CTC CGG TGA GCT GTT GTA AA-3′ (Grx1-reverse), and for mouse DJ-1 were 5′-ATG GCT TCC AAA AGA GCT CTG GT-3′ (DJ-1-forward) and 5′-CCT TAG CCA GTG GGT GTG TT-3′ (DJ-1-reverse). 18S rRNA was used as internal control for normalization. Quantitative real time PCR was performed to confirm knockdown of Grx1 in each experiment and the average

knockdown obtained in all experiments is represented in Figure 2B.

Immunoblot analyses

At the completion of the experiment, cells were washed with PBS and treated with lysis buffer (PBS containing 0.5% Igepal, 1 m*M* EDTA with protease inhibitors). Protein concentration was estimated and the lysates were subjected to SDS-PAGE using 14% (w/v) acrylamide gels. About 20–30 μg of protein was loaded per lane. After electrophoresis the proteins were transferred to PVDF membrane and incubated with the primary antibody (Grx1/DJ-1/SOD1/Trx/FLAG), followed by incubation with appropriate secondary anti-IgG labeled with either alkaline phosphatase or horseradish peroxidase. Immunostained bands were detected using nitroblue tetrazolium and 5-bromo-4-chloro-3-indolyl phosphate as chromogens or using chemiluminescence kit (ECL, Amersham Pharmacia Biotech, France). β-Tubulin levels were measured as loading control for normalization of blots (unless stated otherwise) and used for densitometric analyses accompanying representative blots in figures.

Determination of redox state of FLAG-tagged WT human DJ-1 in Grx1 knocked down cells

Cell lysates prepared as mentioned above were derivatized with 4-acetamido-4′-maleimidylstilbene-2,2′-disulfonic acid, disodium salt (AMS; Invitrogen; 30 m*M*) in Tris buffer (20 m*M*, pH 7.4) at 25°C for 1 h under vacuum and subjected to nonreducing SDS-PAGE as described earlier (41). The samples that were not derivatized with AMS were subjected to both nonreducing and reducing SDS-PAGE, followed by immunoblotting using antibody to FLAG.

Cell death assay

Cells were plated in chamber slides and cell death was assessed at the end of the experimental period using the terminal deoxynucleotidyl transferase mediated dUTP-biotin nick end-labeling (TUNEL) method, following the manufacturer's protocol. The cells were observed using fluorescence microscopy and both TUNEL positive cells and DAPI stained nuclei were counted in four independent experiments in each case. On average, 300 cells were scored over several fields for each sample.

Statistical analyses

Statistical analysis was performed using one-way analysis of variance (ANOVA) followed by Student–Newman–Keuls or Dunnett's test, or Student's *t* test, as appropriate. Values are represented as mean $\pm$ SD (unless stated otherwise) and $p < 0.05$ was considered as statistically significant.

Results

Downregulation of Grx1 causes post-translational decrease of DJ-1 whereas its mRNA levels are unaltered

Knockdown of Grx1 by pAAV-GFP-shRNA and mU6-shRNA in Neuro-2a cells resulted in decrease in DJ-1 protein, as observed by immunocytochemistry (Fig. 1A), and by immunoblotting, respectively (Fig. 1B), as opposed to when empty vector or scrambled sequence was used. mRNA levels of DJ-1 were unaltered, indicating that Grx1 silencing did not result in transcriptional downregulation of DJ-1 (Fig. 1C). Similar depletion of DJ-1 protein in response to Grx1 knockdown was also found in COS-7 and SH-SY5Y cells, indicating a pan-cell type phenomenon (Fig. 1D). Progressive loss of DJ-1 protein was observed in a time-dependent (Fig. 1E; inset shows Grx1 mRNA levels) and transgene dose-dependent manner (Fig. 1F).

Knockdown of glutaredoxin 1 generates reactive oxygen species

Grx1 was downregulated by transiently transfecting Neuro-2a for 72 h with empty vector or pAAV-GFP-shRNA and the knockdown was verified by immunocytochemistry (Fig. 2A). Cells were also transfected with mU6-shRNA to Grx1 and downregulation of Grx1 expression was assessed by qRT-PCR (Fig. 2B) and immunoblotting (Fig. 2C). Whereas Grx1 was consistently silenced by 50%–60 % using shRNA to Grx1, levels of Grx1 were unaffected when cells were transfected with empty vector (Fig. 2B) or scrambled construct. Grx1 knockdown resulted in increased generation of ROS as observed by H_2DCFDA (2′,7′-dichlorodihydrofluorescein-diacetate) staining (Fig. 2D) and quantitative fluorimetric assay of intracellular ROS (Fig. 2E).

Loss of DJ-1 does not occur following glutathione depletion and is not prevented by antioxidants following Grx1 knockdown

In order to investigate if loss of DJ-1 was a ubiquitous downstream consequence of thiol perturbation, we examined DJ-1 status following depletion of glutathione (GSH) using BSO, an inhibitor of γ-glutamylcysteine synthetase, the rate limiting enzyme for GSH synthesis. Total GSH levels dropped by 95% with BSO treatment (Fig. 3A) but GSH loss did not lead to significant change in protein (Fig. 3B) or mRNA (Fig. 3C) levels of Grx1. However, it enhanced the generation of ROS (Fig. 3D) similar to that observed after Grx1 downregulation. Further, treatment with BSO did not cause any alteration in protein levels of DJ-1 (Fig. 3E), indicating that decrease in DJ-1 protein levels is specific to Grx1 downregulation. To further explore if loss of DJ-1 protein in response to Grx1 knockdown is mediated by subsequent ROS generation, the cells were treated with thiol antioxidants α-lipoic acid (ALA; 100 μM) or N-acetyl cysteine (NAC; 0.5 m*M* and 1 m*M*) 6 and 48 h post-transfection, respectively. Depletion of DJ-1 caused by knockdown of Grx1 could not be prevented by either ALA (Fig. 3F) or NAC (Fig. 3G), clearly indicating that loss of DJ-1 is not due to ROS generated by Grx1 knockdown.

Both silencing of Grx1 and glutathione depletion generate oxidative stress and induce upregulation of stress responsive genes

Stress elicited by an oxidative insult is regulated by intracellular compensatory mechanisms as reported earlier (38). Thioredoxin system helps in maintaining redox status of proteins and cytosolic superoxide dismutase 1 (SOD1) defends the cells against oxidative damage by superoxide. SOD1 (Fig. 4A) and Trx (Fig. 4B) protein levels were elevated in mU6-shRNA transfected samples when compared to control.

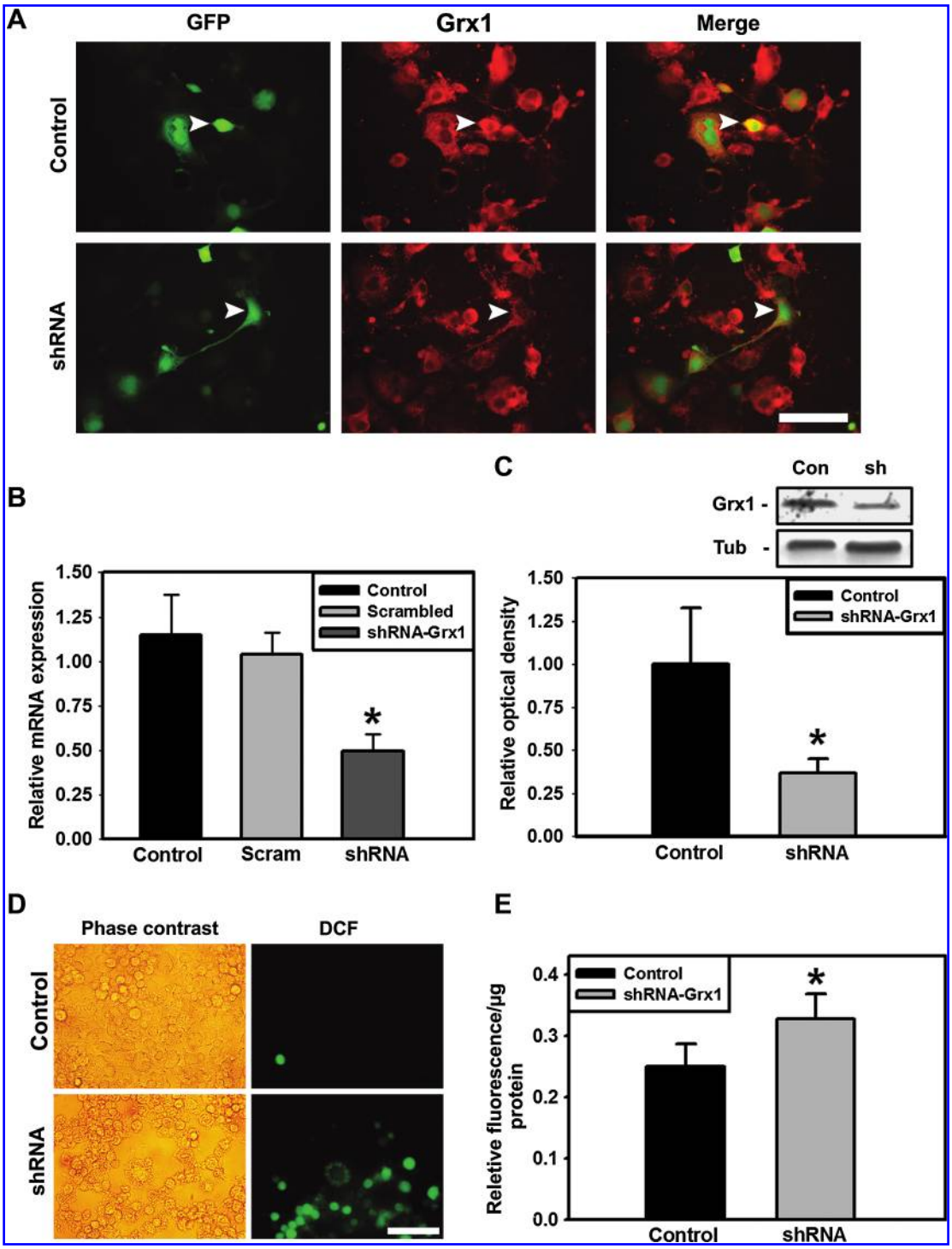

FIG. 2. Knockdown of Grx1 using shRNA generates reactive oxygen species. (**A**) Neuro-2a cells transfected with pAAV-GFP (control) or pAAV-GFP-shRNA (shRNA to Grx1) were immunostained for Grx1. GFP expression represents transfected cells with respective constructs. *Bar* represents 100 μm. (**B**) qRT-PCR depicting Grx1 mRNA levels from Neuro-2a cells transfected with mU6-shRNA or scrambled to Grx1 or empty vector ($n = 4$; $p < 0.005$). (**C**) Representative immunoblot showing Grx1 protein levels in cells transfected with mU6pro vector or shRNA-Grx1. ($n = 6$; $p < 0.01$). (**D, E**) Neuro-2a cells transfected with mU6-shRNA-Grx1 or empty vector were loaded with H_2DCFDA and imaged to examine DCF fluorescence or processed for quantitating DCF fluorescence using fluorimetry ($n = 9$; $p < 0.001$). shRNA to Grx1 enhances ROS generation as observed by (**D**) imaging or (**E**) measurement by fluorimetry. (For interpretation of the references to color in this figure legend, the reader is referred to the web version of this article at www.liebertonline.com/ars).

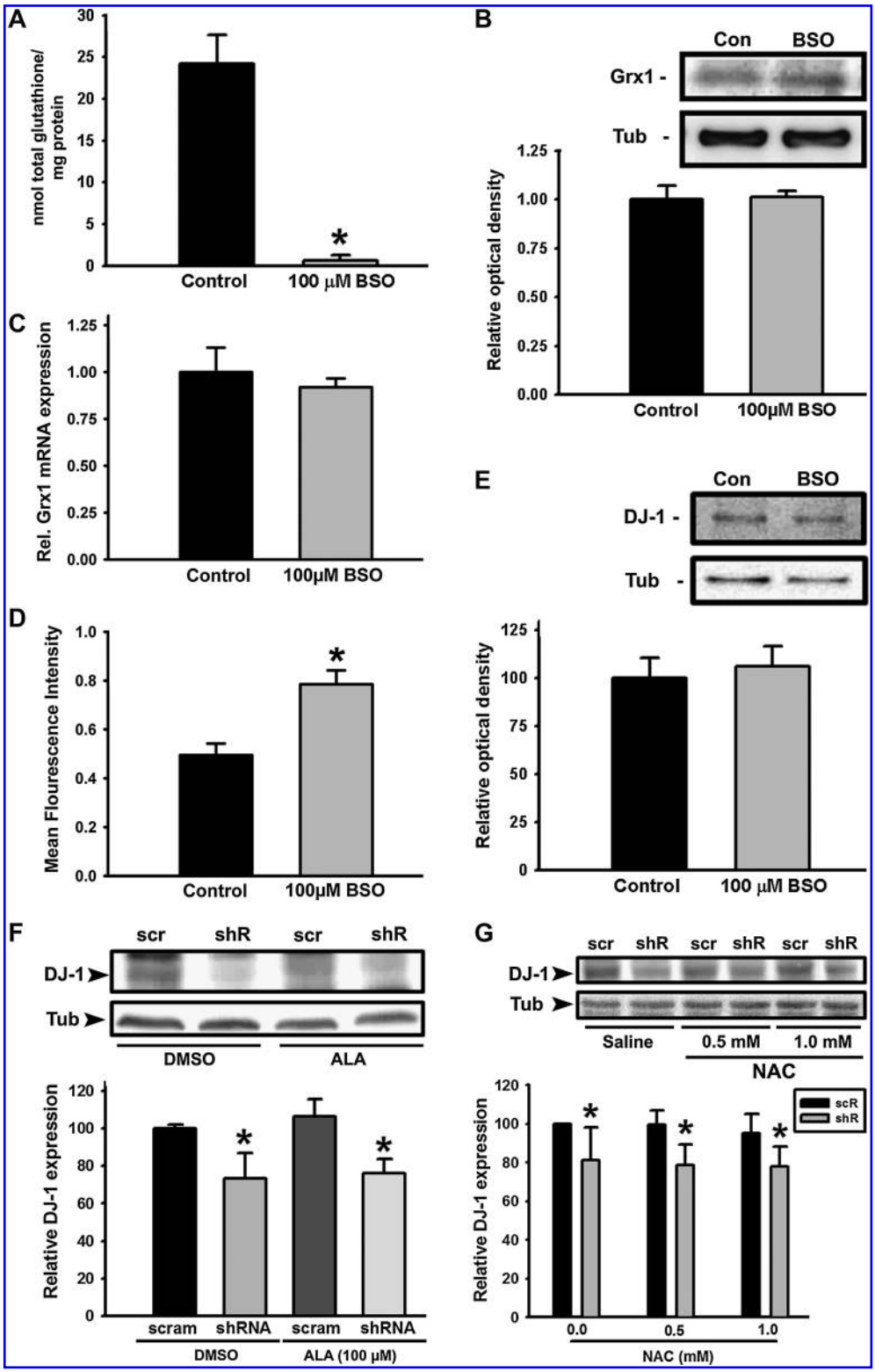

FIG. 3. GSH depletion generates ROS but does not alter DJ-1 protein levels and loss of DJ-1 caused by Grx1 knockdown is not protected by thiol antioxidants. Neuro-2a cells treated with 100 μM BSO or vehicle for 48 h were processed for GSH estimation, qRT-PCR, or immunoblotting. Cells were also processed for ROS measurement. (**A**) Cells treated with BSO show $\sim$95% depletion of GSH as compared to vehicle-treated control ($n = 6$; $p < 0.001$). (**B**) Representative immunoblot shows similar protein levels of Grx1 in cells treated with either BSO (100 μM) or vehicle ($n = 3$). (**C**) BSO treatment does not cause any alteration in the mRNA levels of Grx1 as observed by qRT-PCR ($n = 4$), but (**D**) generates ROS significantly ($n = 12$; $p < 0.001$). (**E**) Representative immunoblot shows no difference in DJ-1 protein from cells treated with BSO (100 μM) or vehicle ($n = 7$). (**F, G**) Neuro-2a cells transfected with shRNA-Grx1 were treated with ALA (100 μM) or NAC (0.5 and 1.0 mM). Loss of DJ-1 protein caused by Grx1 downregulation could not be prevented by (**F**) ALA ($n = 3$; $p = 0.004$) or (**G**) NAC ($n = 6$; $p < 0.01$).

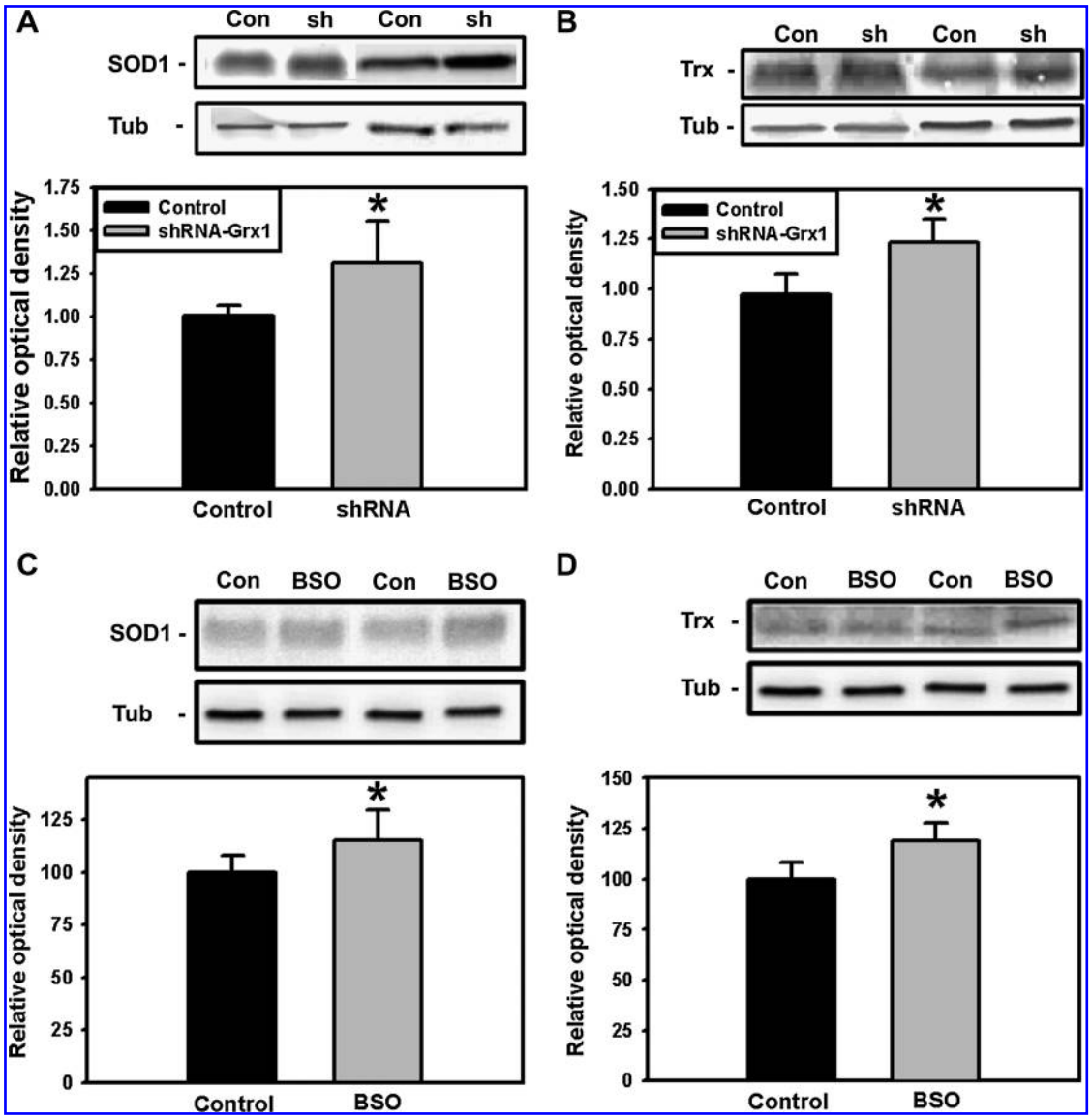

FIG. 4. GSH depletion and Grx1 downregulation both trigger induction of stress responsive proteins. Neuro-2a cells were transfected with shRNA to Grx1 or empty vector and protein levels of SOD1 and Trx were assessed. (**A, B**) shRNA to Grx1 (sh) induces (**A**) SOD1 ($n = 10$; $p = 0.007$) and (**B**) Trx expression ($n = 12$; $p < 0.001$). (**A, B**) Representative immunoblot show increased protein levels of SOD1 and Trx in cells transfected with shRNA to Grx1 as compared to empty vector transfected control, and the same is represented by densitometric analysis. (**C, D**) Protein levels of SOD1 (**C**, $n = 9$; $p = 0.015$) and Trx (**D**, $n = 7$; $p = 0.001$) were similarly induced in lysates from Neuro-2a cells treated with BSO (100 μM) compared with vehicle treated controls as depicted by representative immunoblot.

A similar response was seen in cells treated with 100 μM BSO wherein both SOD1 (Fig. 4C) and Trx (Fig. 4D) levels were increased when compared to control. This suggests that SOD1 and Trx upregulation are part of a general antioxidant defense response that is triggered by both downregulation of Grx1 and depletion of GSH.

Translocation of DJ-1 to mitochondria is specific to Grx1 downregulation and does not occur after GSH depletion

DJ-1 is normally localized both in cytosol and nucleus but translocates to mitochondria following oxidative insult (21, 28). We examined subcellular localization of DJ-1 in response to decreased levels of Grx1 and found that DJ-1 colocalized with MitoTracker, suggesting its translocation to mitochondria (Fig. 5A). This was specific to Grx1 knockdown and did not happen when GSH was depleted (Fig. 5B), implying that translocation of DJ-1 to mitochondria is specifically elicited by downregulation of Grx1 and not by GSH depletion. This was validated by immunoblotting experiments that showed DJ-1 levels to be enriched in mitochondrial fraction of cells with Grx1 knockdown (Fig. 5C).

Silencing of Grx1 results in translocation of Daxx to the cytosol and induces cytotoxicity, a phenomenon not triggered by GSH depletion

DJ-1 sequesters Daxx, a transcriptional repressor within the nucleus under normal physiological conditions (22,

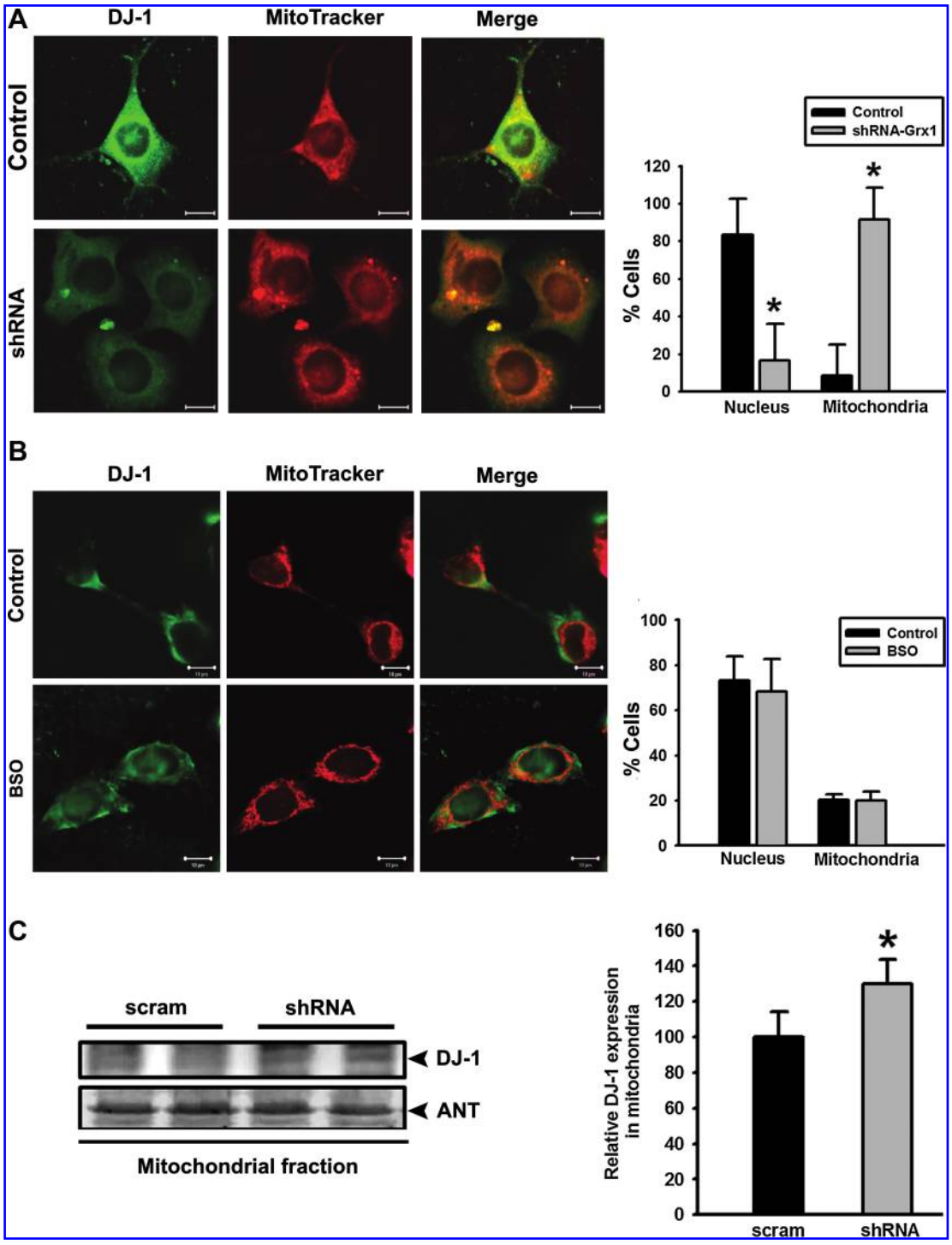

FIG. 5. Grx1 downregulation and not GSH depletion causes mitochondrial translocation of DJ-1. (**A, B**) Neuro-2a cells transfected with shRNA to Grx1 or empty vector or treated with either BSO or vehicle were loaded with MitoTracker, immunostained for DJ-1 and imaged using confocal microscopy. (**A**) shRNA to Grx1 caused depletion of cytosolic and nuclear DJ-1 and triggered its translocation to mitochondria unlike cells transfected with empty vector. Quantification represents percentage of cells showing nuclear retention and mitochondrial translocation of DJ-1 per total number of cells as represented by MitoTracker staining ($n = 4$; $p = 0.003$). (**B**) BSO (100 μM) or vehicle treatment did not trigger mitochondrial translocation of DJ-1 as illustrated by the representative image and quantitation ($n = 4$). *Bar* represents 10 μm. (**C**) Mitochondrial fraction from Neuro-2a cells transfected with shRNA to Grx1 shows enrichment of DJ-1 levels as seen by immunoblot analysis ($n = 4$; $p = 0.02$). Adenine nucleotide translocase (ANT) was used as the mitochondrial loading control. (For interpretation of the references to color in this figure legend, the reader is referred to the web version of this article at www.liebertonline.com/ars).

42, 49). Daxx translocates to the cytosol in response to oxidative stimulus, thereby propagating the cell death cascade (22). Downregulation of Grx1 leads to loss of nuclear DJ-1 and translocation of Daxx (in ~87 % cells with respect to cells transfected with empty vector) from nucleus to cytosol (Fig. 6B). Grx1 downregulation also resulted in cell death (~60%) as inferred by TUNEL assay (Fig. 6A). GSH depletion did not trigger either cytosolic translocation of Daxx (Fig. 6D) or cytotoxicity (Fig. 6C) as compared to vehicle-treated controls. Therefore, Grx1 silencing alone causes translocation of Daxx and subsequent cytotoxicity.

Overexpressed WT human DJ-1 prevents Daxx translocation and abolishes cytotoxicity

We overexpressed WT human DJ-1 in cells wherein Grx1 was silenced and found that human DJ-1 was also lost; in fact to a greater extent than the constitutive mouse DJ-1 (Fig. 7A). Further, overexpression of WT human DJ-1 abolished the cytotoxicity caused by Grx1 downregulation (Fig. 7B). Also, Daxx translocation was completely eliminated by overexpression of WT DJ-1 (Fig. 7C), indicating that in spite of the loss of overexpressed DJ-1, small increment in DJ-1 protein could afford effective protection.

DJ-1 mutants are unaffected by Grx1 knockdown and do not afford cytoprotection thereafter

To elucidate the critical role of cysteine residues underlying DJ-1 depletion in response to Grx1 knockdown, we cotransfected Neuro-2a cells with DJ-1 mutants, such as C106A, C53A and also L166P (a PD pathogenic mutation), along with shRNA to Grx1 or scrambled sequence. Grx1 downregulation did not affect levels of DJ-1 mutants unlike that observed with wild-type DJ-1 (Fig. 8A), suggesting that cysteine residues were involved mechanistically in the loss of DJ-1. Further, these mutants did not offer any cytoprotection and TUNEL-positive cells remained unaffected. Only WT DJ-1 could reverse cytotoxicity caused by Grx1 downregulation (Fig. 8B). Expression of the recombinant mutant of DJ-1, L166P was very low (Fig. 8A), in agreement with earlier reports (34). L166P also caused massive cytotoxicity by itself and when coupled with shRNA to Grx1, the toxicity was further exacerbated leading to loss of cells during the experiment, thus rendering it technically impossible to proceed with the experiment.

Thiol groups of DJ-1 are oxidatively modified in response to Grx1 knockdown

To verify if oxidative modification of thiol groups is the causative factor of loss of DJ-1 protein, we examined redox status of recombinant WT DJ-1 by derivatizing the thiol groups with AMS, a thiol alkylating agent. Both total WT DJ-1 and AMS derivatized WT DJ-1 signals were significantly reduced in cells wherein Grx1 was knocked down when compared to controls. Further, the ratio of AMS derivatized to total WT DJ-1 did not change in Grx1 knockdown compared to control (Fig. 9), indicating that oxidatively modified DJ-1 was degraded rapidly and intact protein was essentially present in reduced form in the cell.

Constitutive DJ-1 is degraded by proteolysis while overexpressed human DJ-1 is degraded by both proteolysis and proteasome

No accumulation of DJ-1 was found in cells treated with MG132, the proteasome inhibitor, in either scrambled or shRNA transfected cells, thus demonstrating that proteasomal degradation is not involved in depletion of constitutive DJ-1 (Fig. 10A). However, overexpressed FLAG-tagged WT human DJ-1 accumulated significantly following inhibition of the proteasome degradation machinery by MG132 (Fig. 10B). Accumulation of β-catenin levels in cells treated with MG132 for 7 h confirmed the inhibition of proteasome (25). In order to determine if proteases were involved in degradation of DJ-1, we inhibited proteases in live cells using a combination of protease inhibitors for 48 h. Cells treated with protease inhibitors were protected from the Grx1 knockdown-mediated loss of DJ-1 protein (Fig. 10C). This suggests that constitutive DJ-1 is degraded by protease(s) following oxidative modification caused by Grx1 knockdown. To further confirm this result, FLAG-tagged WT human DJ-1 construct was coexpressed with mU6-shRNA or scrambled to Grx1 for 48 h, along with protease inhibitors in the medium. FLAG-tagged DJ-1 levels were only partially protected upon inhibiting cellular proteases (Fig. 10D).

Discussion

We describe a pan-cell type phenomenon wherein levels of DJ-1, a key antioxidant protein are lowered by knockdown of Grx1, a TDOR but not by a more global challenge caused by GSH depletion. This is surprising given that DJ-1 is a stress response protein that is upregulated under a variety of cellular stress models (27, 28, 43). The loss of DJ-1 protein is post-translational since DJ-1 mRNA levels were unaffected. The two models used in this study to generate oxidative stress have certain similar features, such as generation of ROS and induction of antioxidant genes (10, 14), but differ in their downstream events, such as depletion of DJ-1 and translocation of DJ-1 and Daxx from the nucleus.

DJ-1 is translocated to the mitochondria when exposed to oxidative challenge, such as rotenone, MPP^+, or H_2O_2, and while this is considered to be protective, the actual mechanism is yet to be clearly understood (1, 8, 21). We looked at the subcellular localization of DJ-1 in both models and strikingly again found a differential response wherein Grx1 knockdown alone led to mitochondrial translocation of residual DJ-1.

DJ-1 sequesters the death-associated protein, Daxx, in the nucleus in promyelocytic leukemia (PML) bodies, preventing it from activating the ASK1-mediated and other cell death pathways in the cytosol (22). Consistent with this role of DJ-1, we found increased amount of Daxx in cytosol following Grx1 knockdown that could be reversed by expressing WT DJ-1 ectopically. Even though the levels of overexpressed WT human DJ-1 were lowered when Grx1 was downregulated, residual overexpressed DJ-1 was sufficient to augment the constitutive levels and afford protection. Nuclear localization of Daxx was unaffected by BSO. The role of Daxx in cell death and its action following translocation has been a matter of debate (22, 40, 49, 51). However, results presented herein demonstrate that translocation of Daxx to cytosol from the nucleus occurs only when nuclear DJ-1 levels decrease. Thus,

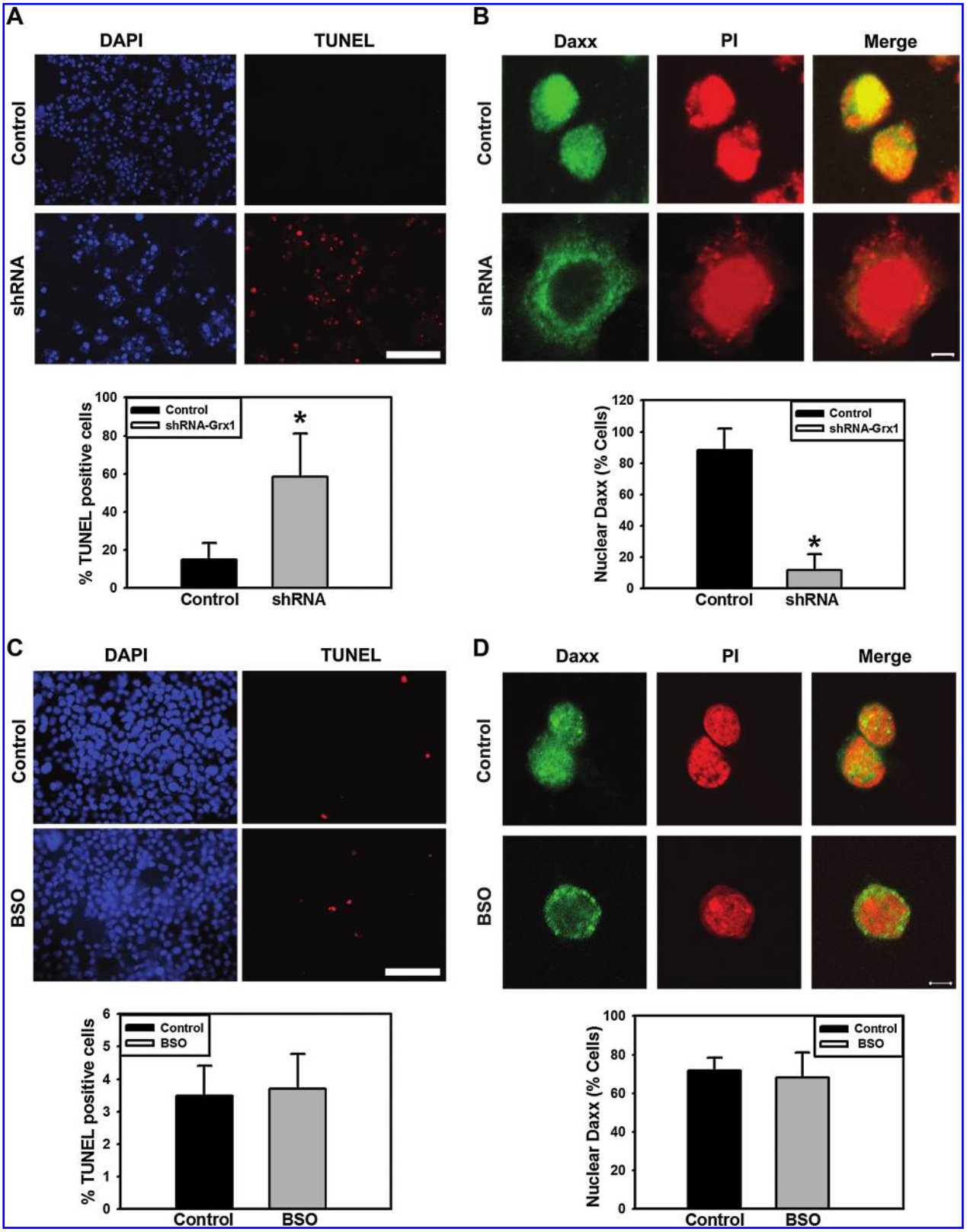

FIG. 6. Daxx translocation and cytotoxicity are triggered by Grx1 knockdown but not by GSH depletion. Neuro-2a cells transfected with shRNA to Grx1 or empty vector or treated with BSO or vehicle were fixed 72 and 48 h later, respectively, and processed for TUNEL assay or immunostaining for Daxx. (**A, B**) Cells transfected with shRNA to Grx1 show significant (**A**) cytotoxicity and (**B**) cytosolic translocation of Daxx as compared to controls. Quantification represents (**A**, $n = 3$; $p = 0.027$) percentage of cells positive for TUNEL staining per total number of DAPI stained nuclei and (**B**, $n = 4$; $p < 0.001$) percentage of cells showing cytosolic translocation of Daxx per total number of cells as represented by PI staining. (**C, D**) BSO treatment to cells (C) neither induced cytotoxicity (**D**) nor triggered cytosolic translocation of Daxx similar to vehicle treated controls ($n = 6$). *Bar* represents 200 μm for **A** and **C** and 10 μm for **B** and **D**. (For interpretation of the references to color in this figure legend, the reader is referred to the web version of this article at www.liebertonline.com/ars).

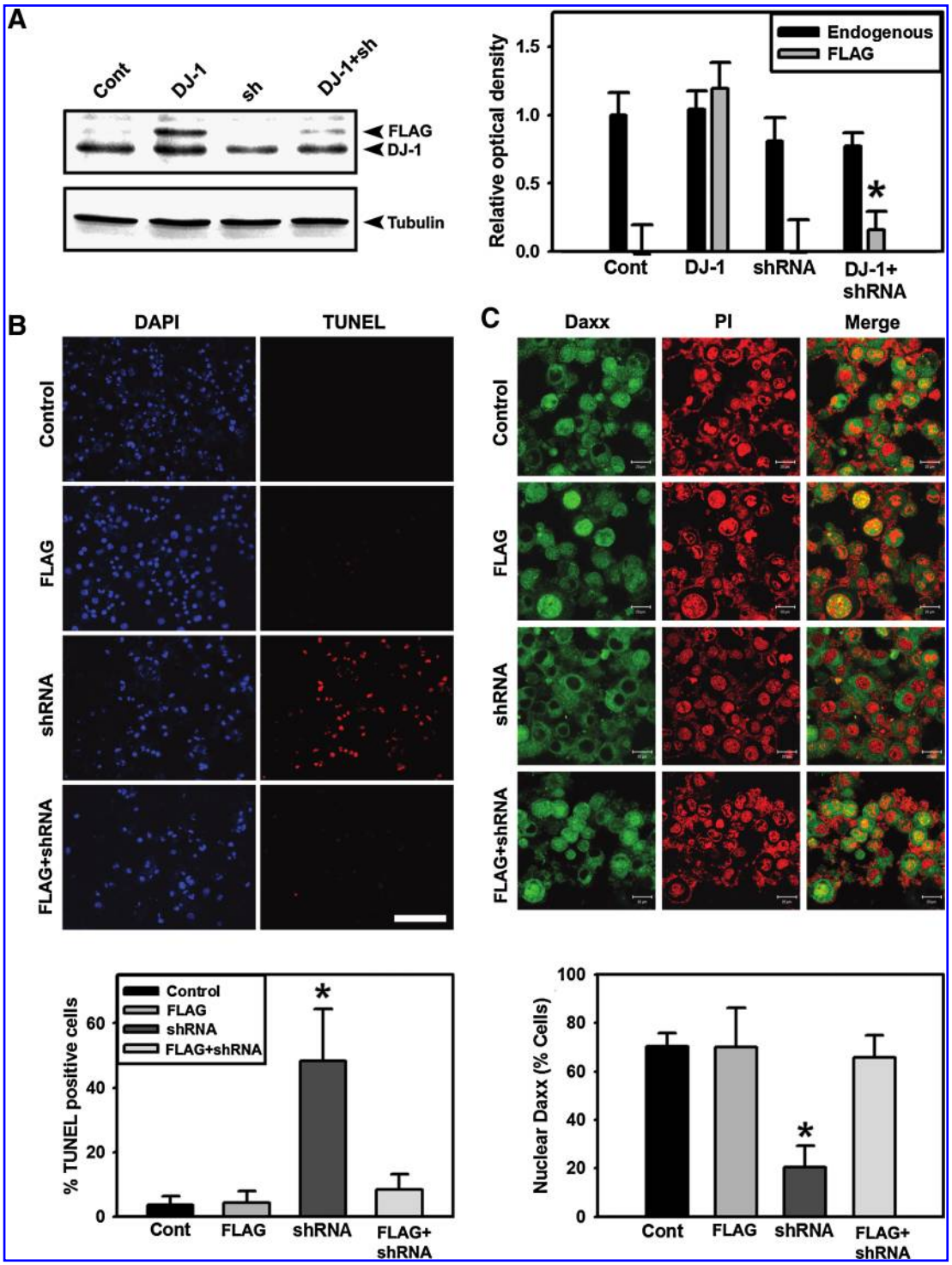

FIG. 7. Overexpression of WT human DJ-1 prevents Daxx translocation and subsequent cytotoxicity. Neuro-2a cells were co-transfected with DJ-1 along with shRNA to Grx1 (sh) or scrambled (Cont) construct and processed for (**A**–**C**) immunoblotting, TUNEL assay, and immunostaining for Daxx. (**A**) shRNA to Grx1 depletes overexpressed DJ-1 protein as seen in representative immunoblot and densitometric analysis ($n = 4$; $p < 0.001$). (**B, C**) Overexpression of DJ-1 (**B**) abolishes cytotoxicity and (**C**) prevents translocation of Daxx mediated by shRNA to Grx1. Quantification represents (**B**) percentage of cells positive for TUNEL staining per total number of DAPI stained nuclei ($n = 10$; $p < 0.05$) and (**C**) percentage of cells showing cytosolic translocation of Daxx per total number of cells as represented by PI staining ($n = 8$; $p < 0.001$). *Bar* represents 200 μm for **B** and 20 μm for **C**. (For interpretation of the references to color in this figure legend, the reader is referred to the web version of this article at www.liebertonline.com/ars).

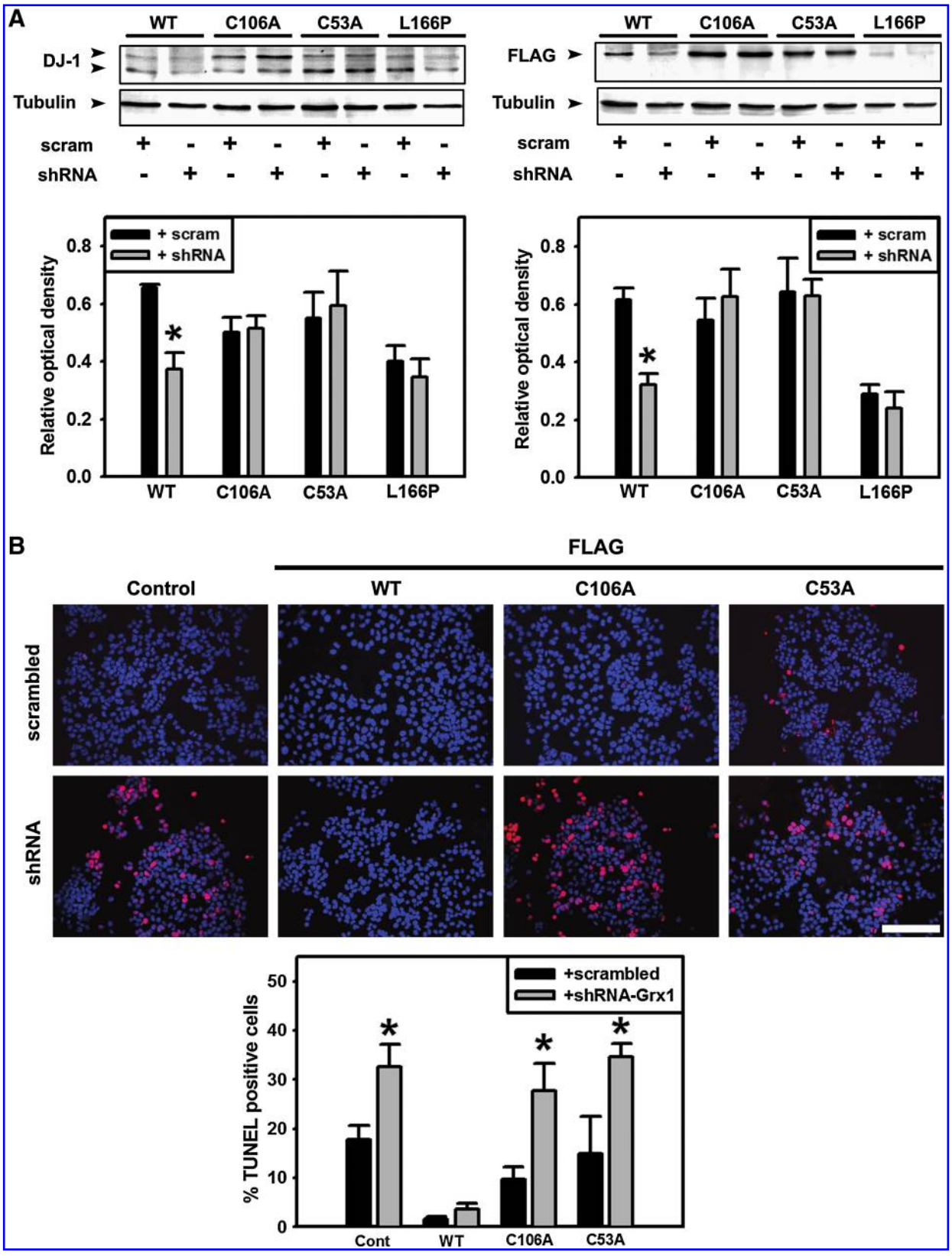

FIG. 8. Cysteine DJ-1 mutants are not affected by Grx1 knockdown and fail to prevent ensuing cytotoxicity. Neuro-2a cells were cotransfected with WT or mutants of DJ-1 (C106A, C53A, L166P) along with shRNA to Grx1 or scrambled construct and processed for immunoblotting or TUNEL assay. (**A**) shRNA to Grx1 did not affect the protein levels of mutants but WT DJ-1 levels were decreased as represented by immunoblots probed with antibody to DJ-1 (*left*, $n = 4$; $p < 0.001$) and anti-FLAG antibody (*right*, $n = 4$; $p = 0.002$) and respective densitometric analysis. (**B**) Mutants of DJ-1 do not protect from cytotoxicity caused by shRNA to Grx1. Quantification represents percentage of cells positive for TUNEL staining per total number of DAPI stained nuclei ($n = 7$; $p < 0.05$). Values are mean ± SEM. Bar represents 200 μm. (For interpretation of the references to color in this figure legend, the reader is referred to the web version of this article at www.liebertonline.com/ars).

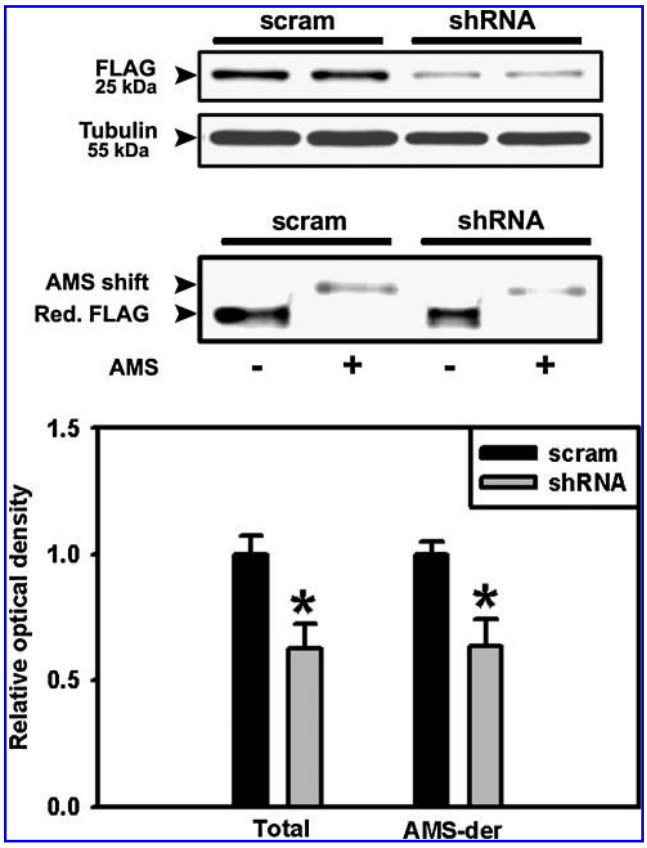

FIG. 9. Grx1 downregulation causes oxidative modification of FLAG-tagged wild-type human DJ-1. Cell lysates from Neuro-2a cells cotransfected with WT DJ-1 and shRNA or scrambled to Grx1 constructs were incubated with AMS and subjected to SDS-PAGE under reducing/nonreducing conditions. Immunoblot depicting total FLAG-tagged WT human DJ-1 and tubulin in cells transfected with shRNA or scrambled to Grx1 electrophoresed under reducing conditions (*upper blot set*), also reduced and AMS derivatized FLAG-tagged protein electrophoresed under non-reducing conditions (*lower blot*). Densitometric analysis depicts total FLAG-tagged protein signals normalized with β-tubulin and AMS derivatized FLAG-tagged DJ-1 signals normalized with total FLAG-tagged protein ($n = 6$; $p < 0.05$). Values are mean ± SEM.

cytosolic translocation of Daxx is dependent on loss of nuclear DJ-1 either by export from nucleus or by degradation. The above events were accompanied by cell death only when Grx1 was downregulated but not by GSH depletion. This is in concurrence with earlier reports using BSO (39). Overexpression of human WT DJ-1 prevented Daxx translocation and was cytoprotective measured as TUNEL positive cells.

DJ-1 has three critical cysteine residues at amino acid positions 46, 53, and 106. Since these residues are known (8, 26, 31, 49) to play an important role in the antioxidant function of DJ-1 and Grx1 functioning as a TDOR can potentially act on these cysteine residues, we examined the status of DJ-1 mutants following Grx1 knockdown. The cysteine mutants (C53A and C106A) did not show any loss in response to Grx1 knockdown (Fig. 8), indicating that the cysteine residues play a critical role in the loss of DJ-1. Oxidative modification of these residues that could potentially occur during Grx1 knockdown may adversely affect stability of the protein resulting in its degradation. Thus, both cysteine residues at 53 and 106 positions are critical for cellular protection under the current experimental paradigm.

DJ-1 could potentially be glutathionylated under decreased Grx1 levels, a phenomenon probably not seen with GSH depletion. We examined the redox status of DJ-1 in response to Grx1 knockdown and found that intact DJ-1 in the cells was essentially present in the reduced form since there was a proportional decrease in the reduced fraction of DJ-1 with a loss in total protein levels. This suggests that oxidatively modified DJ-1 is rapidly degraded and the intact DJ-1 in cells is present principally in the reduced form.

During oxidative stress, as a first step DJ-1 is presumably oxidized to sulfenic acid at the critical cysteines in both the paradigms used in this study (32, 48). Sulfenic acids can then form mixed disulfides with GSH or other protein thiol(s), reactions catalyzed by TDORs including Trx and Grx. Grx1 would then potentially play a critical role in deglutathionylation of DJ-1. In the absence of Grx1 and replete cellular GSH, glutathionylated DJ-1 would accumulate in this experimental paradigm, which presumably undergoes translocation (4, 8) and degradation. Given that GSH levels are depleted following BSO, the sulfenic acids are possibly transformed predominantly to protein mixed disulfides (Pr-SS-Pr) and also to Pr-SSG. Thus, the presence of Grx1 may be critical to reverse glutathionylation of DJ-1 thereby preventing its degradation. During GSH depletion, protein thiol pools along with TDORs may help in maintaining the reduced status of DJ-1 (Supplemental Fig. 1; see www.liebertonline.com/ars).

In order to further understand the mechanism underlying loss of DJ-1, we inhibited the ubiquitin–proteasome machinery and cellular proteases and examined the DJ-1 status. DJ-1 has been reported to undergo cleavage at the 157/158 amino acid residues through a proteolytic mechanism when subjected to a strong oxidative stimulus such as H_2O_2 (36). Interestingly, inhibiting cellular proteases with a combination of protease inhibitors abolished loss of constitutive DJ-1 caused by Grx1 knockdown (Fig. 10C). However, overexpressed FLAG-tagged DJ-1 loss could be attenuated by proteasome inhibitors (Fig. 10B), indicating that constitutive and overexpresssed proteins were processed by separate mechanisms following their oxidative modification at critical cysteine residues. It has also been shown that DJ-1 can act as a protease in a cell-free system (18, 20, 35). This suggests that oxidized DJ-1 can undergo autoproteolysis, which might also explain the increased loss of DJ-1 seen following overexpression.

A small decrement of DJ-1 (~25%-30%) triggers a cascade of deleterious responses, indicating the importance of maintaining critical levels of this protein in specific subcellular compartments. Several important cellular functions such as antioxidant (28, 37), transcriptional regulator (12, 15, 50), and chaperone activity (2, 29, 44) have been attributed to DJ-1. Dysfunction or downregulation of DJ-1 potentiates cellular toxicity (7) while overexpression is protective (33, 45). Given that loss of function mutations in DJ-1 are associated with familial PD, the importance of this multifunctional protein cannot be overemphasized. We demonstrate here for the first time that perturbation of protein thiol homeostasis through downregulation of a TDOR, Grx1 can lead to loss of DJ-1 through proteolysis. Downregulation of Grx1 is known to affect mitochondrial complex I activity and increase vulnerability to SNpc cell loss in animal model of PD (16, 23, 24) and

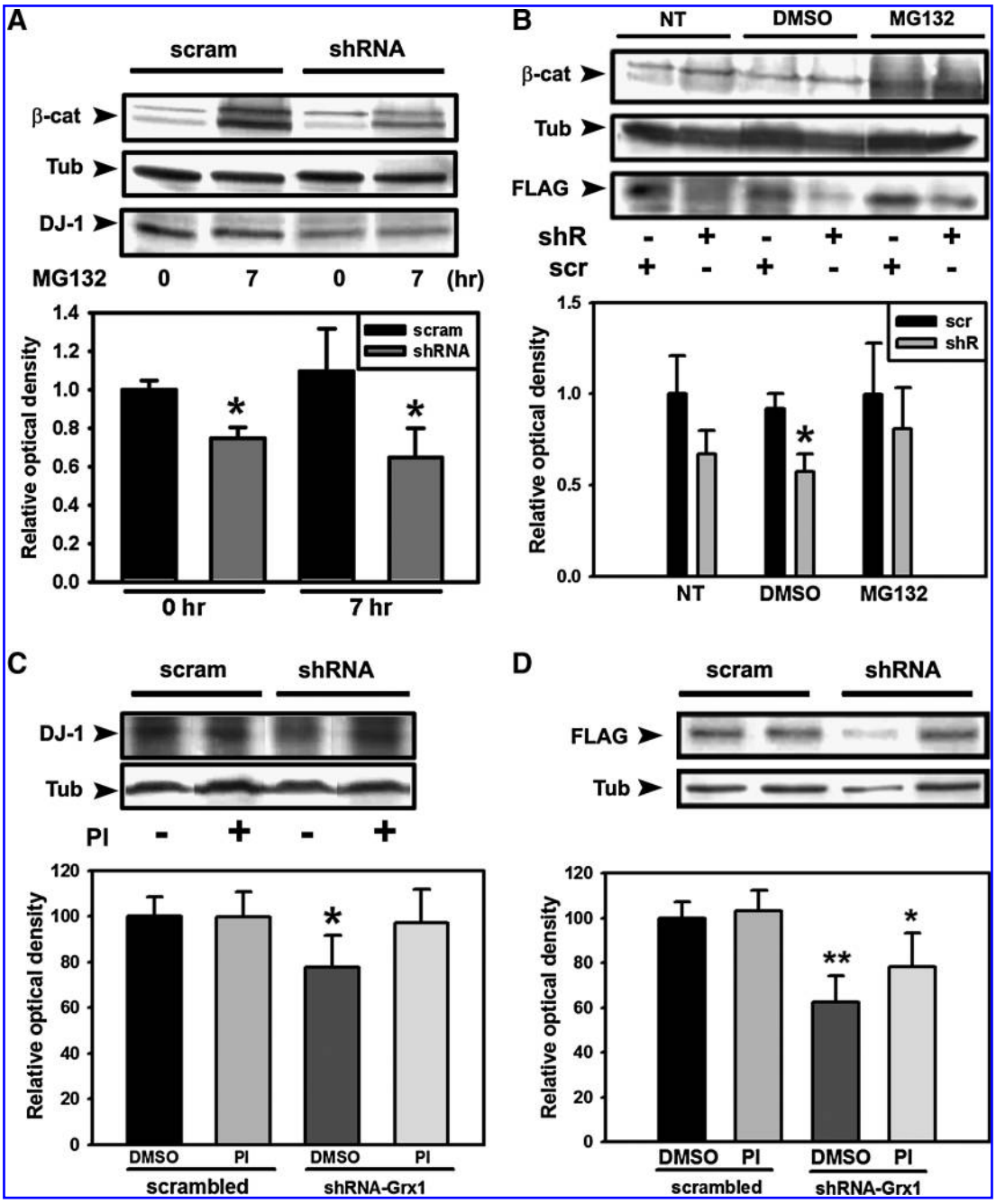

FIG. 10. Constitutive DJ-1 is degraded by proteolysis while overexpressed human DJ-1 is degraded by both proteolysis and proteasome. (**A**) Neuro-2a cells were transfected with scrambled or shRNA to Grx1 construct, and treated with MG132 for 0 or 7 h prior to harvesting. Loss of constitutive DJ-1 caused by shRNA to Grx1 is not prevented by MG132, whereas β-catenin accumulates after 7 h treatment ($n = 4$; $p < 0.001$). (**B**) Neuro-2a cells cotransfected with FLAG-tagged WT human DJ-1 and shRNA or scrambled construct were treated with MG132 or DMSO (vehicle) 41 h post-transfection for 7 h. Nontreated (NT) cells were collected at 41 h proceeding transfection. Loss of exogenous DJ-1 caused by shRNA to Grx1 is partially prevented by MG132, whereas β-catenin accumulates after 7 h treatment ($n = 3$; $p < 0.05$) (C) Neuro-2a cells were transfected with scrambled or shRNA to Grx1, and treated with protease inhibitor cocktail for 48 h following transfection. Grx1 knockdown induced loss of DJ-1 is abolished by treatment with protease inhibitors and is comparable to scrambled transfected controls ($n = 8$; $p < 0.01$) (**D**) Neuro-2a cells were transfected with scrambled or shRNA to Grx1 and FLAG-tagged WT human DJ-1, and treated with protease inhibitor cocktail or 0.05% DMSO for 48 h following transfection. Grx1 knockdown induced loss of WT DJ-1 is partially protected by treatment with protease inhibitors ($n = 7$; $^*p = 0.01$ and $^{**}p < 0.001$).

can occur following cadmium exposure (11). Further, DJ-1 loss could also occur during perturbations of protein thiol homeostasis caused by dysfunction of other TDORs, such as thioredoxin. Thus, dysfunction of TDORs may confer susceptibility to sporadic PD through multiple mechanisms, including loss of DJ-1.

Acknowledgments

We thank Bhavana Srivastava and Shailesh K. Gupta for generating the constructs (pAAV-shRNA-Grx1 & pAAV-GFP, respectively). Our kind thanks to Lalitha Durgadoss and Prakash Nidadavolu for their help in some experiments. We acknowledge the assistance of P. Manish. We also thank Dr. Nihar R. Jana for his help. We thank Prof. D. Turner (Univ. Of Michigan, Ann Arbor) for the mU6pro vector and Prof. Tak W. Mak (The Campbell Family Institute for Breast Cancer Research, ON, Canada) and Prof. David S. Park (Univ. of Ottawa, ON, Canada) for the DJ-1 constructs. US and AR were supported by University Grants Commission & Council of Scientific & Industrial Research, India, respectively. The work was partially supported by the J.C. Bose fellowship to VR from the Department of Science & Technology, Government of India.

Authors' contributions: US, AR, and VR conceptualized and designed the experiments. US, AR, RKV, and AMRK performed the experiments and analyzed data. US, AR, and VR wrote the manuscript.

Author Disclosure Statement

The authors declare no conflict of interest.

References

1. Ashley AK, Hanneman WH, Katoh T, Moreno JA, Pollack A, Tjalkens RB, and Legare ME. Analysis of targeted mutation in DJ-1 on cellular function in primary astrocytes. *Toxicol Lett* 184: 186–191, 2009.
2. Batelli S, Albani D, Rametta R, Polito L, Prato F, Pesaresi M, Negro A, and Forloni G. DJ-1 modulates alpha-synuclein aggregation state in a cellular model of oxidative stress: Relevance for Parkinson's disease and involvement of HSP70. *PLoS One* 3: e1884, 2008.
3. Benzi G and Moretti A. Are reactive oxygen species involved in Alzheimer's disease? *Neurobiol Aging* 16: 661–674, 1995.
4. Blackinton J, Lakshminarasimhan M, Thomas KJ, Ahmad R, Greggio E, Raza AS, Cookson MR, and Wilson MA. Formation of a stabilized cysteine sulfinic acid is critical for the mitochondrial function of the parkinsonism protein DJ-1. *J Biol Chem* 284: 6476–6485, 2009.
5. Bonifati V. Genetics of parkinsonism. *Parkinsonism Relat Disord* 13: S233–241, 2007.
6. Bradford MM. A rapid and sensitive method for the quantitation of microgram quantities of protein utilizing the principle of protein-dye binding. *Anal Biochem* 72: 248–254, 1976.
7. Bretaud S, Allen C, Ingham PW, and Bandmann O. p53-dependent neuronal cell death in a DJ-1-deficient zebrafish model of Parkinson's disease. *J Neurochem* 100: 1626–1635, 2007.
8. Canet–Aviles RM, Wilson MA, Miller DW, Ahmad R, McLendon C, Bandyopadhyay S, Baptista MJ, Ringe D, Petsko GA, and Cookson MR. The Parkinson's disease protein DJ-1 is neuroprotective due to cysteine-sulfinic acid-driven mitochondrial localization. *Proc Natl Acad Sci USA* 101: 9103–9108, 2004.
9. Chinta SJ and Andersen JK. Redox imbalance in Parkinson's disease. *Biochim Biophys Acta* 1780: 1362–1367, 2008.
10. Chiueh CC, Andoh T, and Chock PB. Roles of thioredoxin in nitric oxide-dependent preconditioning-induced tolerance against MPTP neurotoxin. *Toxicol Appl Pharmacol* 207: 96–102, 2005.
11. Chrestensen CA, Starke DW, and Mieyal JJ. Acute cadmium exposure inactivates thioltransferase (glutaredoxin), inhibits intracellular reduction of protein–glutathionyl-mixed disulfides, and initiates apoptosis. *J Biol Chem* 275: 26556–26565, 2000.
12. Clements CM, McNally RS, Conti BJ, Mak TW, and Ting JP. DJ-1, a cancer- and Parkinson's disease-associated protein, stabilizes the antioxidant transcriptional master regulator Nrf2. *Proc Natl Acad Sci USA* 103: 15091–15096, 2006.
13. Cotgreave IA, Gerdes R, Schuppe–Koistinen I, and Lind C. S-glutathionylation of glyceraldehyde-3-phosphate dehydrogenase: Role of thiol oxidation and catalysis by glutaredoxin. *Methods Enzymol* 348: 175–182, 2002.
14. Das DK. Thioredoxin regulation of ischemic preconditioning. *Antioxid Redox Signal* 6: 405–412, 2004.
15. Davidson B, Hadar R, Schlossberg A, Sternlicht T, Slipicevic A, Skrede M, Risberg B, Florenes VA, Kopolovic J, and Reich R. Expression and clinical role of DJ-1, a negative regulator of PTEN, in ovarian carcinoma. *Hum Pathol* 39: 87–95, 2008.
16. Diwakar L, Kenchappa RS, Annepu J, and Ravindranath V. Downregulation of glutaredoxin but not glutathione loss leads to mitochondrial dysfunction in female mice CNS: Implications in excitotoxicity. *Neurochem Int* 51: 37–46, 2007.
17. Gallogly MM, Starke DW, and Mieyal JJ. Mechanistic and kinetic details of thiol-disulfide exchange by glutaredoxins and potential mechanisms of regulation. *Antioxid Redox Signal* 11: 1059–1081, 2009.
18. Gorner K, Holtorf E, Odoy S, Nuscher B, Yamamoto A, Regula JT, Beyer K, Haass C, and Kahle PJ. Differential effects of Parkinson's disease-associated mutations on stability and folding of DJ-1. *J Biol Chem* 279: 6943–6951, 2004.
19. Holmgren A. Hydrogen donor system for *Escherichia coli* ribonucleoside-diphosphate reductase dependent upon glutathione. *Proc Natl Acad Sci USA* 73: 2275–2279, 1976.
20. Honbou K, Suzuki NN, Horiuchi M, Niki T, Taira T, Ariga H, and Inagaki F. The crystal structure of DJ-1, a protein related to male fertility and Parkinson's disease. *J Biol Chem* 278: 31380–31384, 2003.
21. Junn E, Jang WH, Zhao X, Jeong BS, and Mouradian MM. Mitochondrial localization of DJ-1 leads to enhanced neuroprotection. *J Neurosci Res* 87: 123–129, 2009.
22. Junn E, Taniguchi H, Jeong BS, Zhao X, Ichijo H, and Mouradian MM. Interaction of DJ-1 with Daxx inhibits apoptosis signal-regulating kinase 1 activity and cell death. *Proc Natl Acad Sci USA* 102: 9691–9696, 2005.
23. Kenchappa RS, Diwakar L, Boyd MR, and Ravindranath V. Thioltransferase (glutaredoxin) mediates recovery of motor neurons from excitotoxic mitochondrial injury. *J Neurosci* 22: 8402–8410, 2002.
24. Kenchappa RS and Ravindranath V. Glutaredoxin is essential for maintenance of brain mitochondrial complex I: Studies with MPTP. *FASEB J* 17: 717–719, 2003.
25. Kim NG, Xu C, and Gumbiner BM. Identification of targets of the Wnt pathway destruction complex in addition to beta-catenin. *Proc Natl Acad Sci USA* 106: 5165–5170, 2009.

26. Kinumi T, Kimata J, Taira T, Ariga H, and Niki E. Cysteine-106 of DJ-1 is the most sensitive cysteine residue to hydrogen peroxide-mediated oxidation *in vivo* in human umbilical vein endothelial cells. *Biochem Biophys Res Commun* 317: 722–728, 2004.
27. Lev N, Ickowicz D, Barhum Y, Lev S, Melamed E, and Offen D. DJ-1 protects against dopamine toxicity. *J Neural Transm* 116: 151–160, 2009.
28. Lev N, Ickowicz D, Melamed E, and Offen D. Oxidative insults induce DJ-1 upregulation and redistribution: Implications for neuroprotection. *Neurotoxicology* 29: 397–405, 2008.
29. Liu F, Nguyen JL, Hulleman JD, Li L, and Rochet JC. Mechanisms of DJ-1 neuroprotection in a cellular model of Parkinson's disease. *J Neurochem* 105: 2435–2453, 2008.
30. Mieyal JJ, Gallogly MM, Qanungo S, Sabens EA, and Shelton MD. Molecular mechanisms and clinical implications of reversible protein S-glutathionylation. *Antioxid Redox Signal* 10: 1941–1988, 2008.
31. Mitsumoto A, Nakagawa Y, Takeuchi A, Okawa K, Iwamatsu A, and Takanezawa Y. Oxidized forms of peroxiredoxins and DJ-1 on two-dimensional gels increased in response to sublethal levels of paraquat. *Free Radic Res* 35: 301–310, 2001.
32. Miyazaki S, Yanagida T, Nunome K, Ishikawa S, Inden M, Kitamura Y, Nakagawa S, Taira T, Hirota K, Niwa M, Iguchi–Ariga SM, and Ariga H. DJ-1-binding compounds prevent oxidative stress-induced cell death and movement defect in Parkinson's disease model rats. *J Neurochem* 105: 2418–2434, 2008.
33. Mo JS, Kim MY, Ann EJ, Hong JA, and Park HS. DJ-1 modulates UV-induced oxidative stress signaling through the suppression of MEKK1 and cell death. *Cell Death Differ* 15: 1030–1041, 2008.
34. Moore DJ, Zhang L, Dawson TM, and Dawson VL. A missense mutation (L166P) in DJ-1, linked to familial Parkinson's disease, confers reduced protein stability and impairs homo-oligomerization. *J Neurochem* 87: 1558–1567, 2003.
35. Olzmann JA, Brown K, Wilkinson KD, Rees HD, Huai Q, Ke H, Levey AI, Li L, and Chin LS. Familial Parkinson's disease-associated L166P mutation disrupts DJ-1 protein folding and function. *J Biol Chem* 279: 8506–8515, 2004.
36. Ooe H, Maita C, Maita H, Iguchi–Ariga SM, and Ariga H. Specific cleavage of DJ-1 under an oxidative condition. *Neurosci Lett* 406: 165–168, 2006.
37. Ooe H, Taira T, Iguchi–Ariga SM, and Ariga H. Induction of reactive oxygen species by bisphenol A and abrogation of bisphenol A-induced cell injury by DJ-1. *Toxicol Sci* 88: 114–126, 2005.
38. Papadia S, Soriano FX, Leveille F, Martel MA, Dakin KA, Hansen HH, Kaindl A, Sifringer M, Fowler J, Stefovska V, McKenzie G, Craigon M, Corriveau R, Ghazal P, Horsburgh K, Yankner BA, Wyllie DJ, Ikonomidou C, and Hardingham GE. Synaptic NMDA receptor activity boosts intrinsic antioxidant defenses. *Nat Neurosci* 11: 476–487, 2008.
39. Park HA, Khanna S, Rink C, Gnyawali S, Roy S, and Sen CK. Glutathione disulfide induces neural cell death via a 12-lipoxygenase pathway. *Cell Death Differ* 16: 1167–1179, 2009.
40. Roubille F, Combes S, Leal–Sanchez J, Barrere C, Cransac F, Sportouch-Dukhan C, Gahide G, Serre I, Kupfer E, Richard S, Hueber AO, Nargeot J, Piot C, and Barrere–Lemaire S. Myocardial expression of a dominant-negative form of Daxx decreases infarct size and attenuates apoptosis in an *in vivo* mouse model of ischemia/reperfusion injury. *Circulation* 116: 2709–2717, 2007.
41. Saeed U, Durgadoss L, Valli RK, Joshi DC, Joshi PG, Ravindranath V. Knockdown of cytosolic glutaredoxin 1 leads to loss of mitochondrial membrane potential: Implication in neurodegenerative diseases. *PLoS One* 3: e2459, 2008.
42. Saeed U, Karunakaran S, Meka DP, Koumar RC, Ramakrishnan S, Joshi SD, Nidadavolu P, and Ravindranath V. Redox activated MAP kinase death signaling cascade initiated by ASK1 is not activated in female mice following MPTP: Novel mechanism of neuroprotection. *Neurotox Res* 16: 116–126, 2009.
43. Sakurai M, Kawamura T, Nishimura H, Suzuki H, Tezuka F, and Abe K. Induction of Parkinson disease-related proteins in motor neurons after transient spinal cord ischemia in rabbits. *J Cereb Blood Flow Metab* 29: 752–758, 2009.
44. Shendelman S, Jonason A, Martinat C, Leete T, and Abeliovich A. DJ-1 is a redox-dependent molecular chaperone that inhibits alpha-synuclein aggregate formation. *PLoS Biol* 2: e362, 2004.
45. Shinbo Y, Niki T, Taira T, Ooe H, Takahashi–Niki K, Maita C, Seino C, Iguchi–Ariga SM, and Ariga H. Proper SUMO-1 conjugation is essential to DJ-1 to exert its full activities. *Cell Death Differ* 13: 96–108, 2006.
46. Sriram K, Shankar SK, Boyd MR, and Ravindranath V. Thiol oxidation and loss of mitochondrial complex I precede excitatory amino acid-mediated neurodegeneration. *J Neurosci* 18: 10287–10296, 1998.
47. Taira T, Saito Y, Niki T, Iguchi-Ariga SM, Takahashi K, and Ariga H. DJ-1 has a role in antioxidative stress to prevent cell death. *EMBO Rep* 5: 213–218, 2004.
48. Tsuboi Y, Munemoto H, Ishikawa S, Matsumoto K, Iguchi–Ariga SM, and Ariga H. DJ-1, a causative gene product of a familial form of Parkinson's disease, is secreted through microdomains. *FEBS Lett* 582: 2643–2649, 2008.
49. Waak J, Weber SS, Gorner K, Schall C, Ichijo H, Stehle T, and Kahle PJ. Oxidizable residues mediating protein stability and cytoprotective interaction of DJ-1 with apoptosis signal-regulating kinase 1. *J Biol Chem* 284: 14245–14257, 2009.
50. Zhong N and Xu J. Synergistic activation of the human MnSOD promoter by DJ-1 and PGC-1alpha: Regulation by SUMOylation and oxidation. *Hum Mol Genet* 17: 3357-33-67, 2008.
51. Zobalova R, Swettenham E, Chladova J, Dong LF, and Neuzil J. Daxx inhibits stress-induced apoptosis in cardiac myocytes. *Redox Rep* 13: 263–270, 2008.

Address correspondence to:
Vijayalakshmi Ravindranath
Centre for Neuroscience
Indian Institute of Science
C.V. Raman Avenue
Bangalore 560012
India

E-mail: viji@cns.iisc.ernet.in

Date of first submission to ARS Central, August 21, 2009; date of final revised submission, December 9, 2009; date of acceptance, December 14, 2009.

Abbreviations Used

ALA = α-lipoic acid
AMS = 4-acetamido-4′-maleimidylstilbene-2, 2′-disulfonic acid, disodium salt
ATP13A2 = ATPase type 13A2
BSO = L-buthionine-S-R-sulfoximine
DAPI = 4′,6-diamidino-2-phenylindole
DMSO = dimethyl sulfoxide
Grx = glutaredoxin
GSH = glutathione/reduced glutathione
GSSG = oxidized glutathione
H_2DCFDA = dichlorodihydrofluorescein diacetate
HtrA2/Omi = high-temperature-regulated A2
Lrrk2 = leucine-rich repeat kinase 2
MPP^+ = 1-methyl-4-phenylpyridinium
NAC = N-acetyl cysteine
PD = Parkinson's disease
PI = propidium iodide
PINK1 = PTEN-induced kinase 1
Pr-SSG = protein-glutathione mixed disulfide
Pr-SS-Pr, = intra/inter-molecular disulfide
SNpc = substantia nigra pars compacta
SOD = superoxide dismutase
TDOR = thiol disulfide oxidoreductase
Trx = thioredoxin
TUNEL = terminal deoxynucleotidyl transferase mediated dUTP-biotin nick end-labeling

This article has been cited by:

1. Humberto Rodriguez-Rocha , Aracely Garcia Garcia , Laura Zavala-Flores , Sumin Li , Nandakumar Madayiputhiya , Rodrigo Franco . Glutaredoxin 1 Protects Dopaminergic Cells by Increased Protein Glutathionylation in Experimental Parkinson's Disease. *Antioxidants & Redox Signaling*, ahead of print. [Abstract] [Full Text HTML] [Full Text PDF] [Full Text PDF with Links] [Supplemental material]
2. Michel Prudent, David Crettaz, Julien Delobel, Jean-Daniel Tissot, Niels Lion. 2012. Proteomic analysis of Intercept-treated platelets. *Journal of Proteomics* . [CrossRef]
3. Aracely Garcia-Garcia , Laura Zavala-Flores , Humberto Rodriguez-Rocha , Rodrigo Franco . Thiol-Redox Signaling, Dopaminergic Cell Death, and Parkinson's Disease. *Antioxidants & Redox Signaling*, ahead of print. [Abstract] [Full Text HTML] [Full Text PDF] [Full Text PDF with Links]
4. Elizabeth A. Sabens Liedhegner , Xing-Huang Gao , John J. Mieyal . 2012. Mechanisms of Altered Redox Regulation in Neurodegenerative Diseases—Focus on S-Glutathionylation. *Antioxidants & Redox Signaling* **16**:6, 543-566. [Abstract] [Full Text HTML] [Full Text PDF] [Full Text PDF with Links]
5. Elizabeth A. Sabens Liedhegner, Kelly M. Steller, John J. Mieyal. 2011. Levodopa Activates Apoptosis Signaling Kinase 1 (ASK1) and Promotes Apoptosis in a Neuronal Model: Implications for the Treatment of Parkinson's Disease. *Chemical Research in Toxicology* 110822121032010. [CrossRef]
6. Ying Xiong , Joachim D. Uys , Kenneth D. Tew , Danyelle M. Townsend . 2011. S-Glutathionylation: From Molecular Mechanisms to Health Outcomes. *Antioxidants & Redox Signaling* **15**:1, 233-270. [Abstract] [Full Text HTML] [Full Text PDF] [Full Text PDF with Links]